

# UC Berkeley

## UC Berkeley Previously Published Works

### Title

Synthetic iron (hydr)oxide-glucose associations in subsurface soil: Effects on decomposability of mineral associated carbon

### Permalink

<https://escholarship.org/uc/item/9fs4378j>

### Authors

Porras, RC  
Pries, CE Hicks  
Torn, MS  
[et al.](#)

### Publication Date

2018-02-01

### DOI

10.1016/j.scitotenv.2017.08.290

Peer reviewed

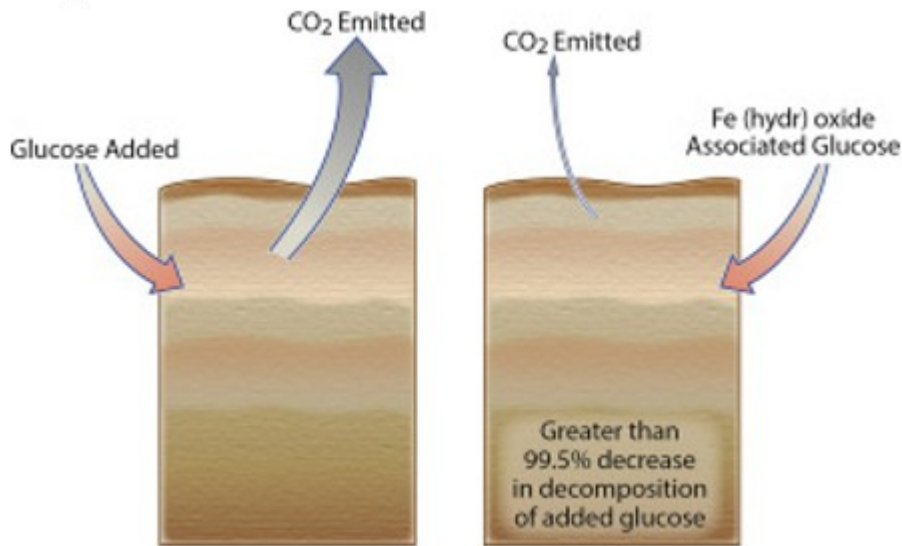
# Synthetic iron (hydr)oxide-glucose associations in subsurface soil: Effects on decomposability of mineral associated carbon

R.C. Porras<sup>a</sup> C.E. Hicks Pries<sup>ab</sup> M.S.Torn<sup>a</sup> P.S.Nico<sup>a</sup>

## Abstract

Soils are a globally important reservoir of organic carbon. There is a growing understanding that interactions with soil mineral phases contribute to the accumulation and retention of otherwise degradable organic matter (OM) in soils and sediments. However, the bioavailability of organic compounds in mineral-organic-associations (MOAs), especially under varying environmental conditions is not well known. To assess the impact of mineral association and warming on the decomposition of an easily respirable organic substrate (glucose), we conducted a series of laboratory incubations at different temperatures with field-collected soils from 10 to 20 cm, 50–60 cm, and 80–90 cm depth. We added <sup>13</sup>C-labeled glucose either directly to native soil or sorbed to one of two synthetic iron (hydr)oxide phases (goethite and ferrihydrite) that differ in crystallinity and affinity for sorbing glucose. We found that: (1) association with the Fe (hydr)oxide minerals reduced the decomposition rate of glucose by > 99.5% relative to rate of decomposition for free glucose in soil; (2) the respiration rate per gram carbon did not differ appreciably with depth, suggesting a similar degree of decomposability for native C across depths and that under the incubation conditions total carbon availability represents the principal limitation on respiration under these conditions as opposed to reduced abundance of decomposers or moisture and oxygen limitations; (3) addition of free glucose enhanced native carbon respiration at all soil depths with the largest effect at 50–60 cm; (4) in general respiration of the organo-mineral complex (glucose and iron-(hydr)oxide) was less temperature sensitive than was respiration of native carbon; (5) the addition of organic free mineral decreased the rate of soil respiration in the intermediate 50–60 cm depth soil. The results emphasize the key role of MOAs in regulating the fluxes of carbon from soils to the atmosphere and in turn the stocks of soil carbon.

Graphical abstract



Keywords: Soil, Organic matter, Mineral association, Decomposition, Glucose, Iron oxide, Iron (hydr)oxide

## 1. Introduction

Soils are a globally important reservoir for carbon and contain upwards of 2000–3000 Pg of carbon (Jobbagy and Jackson, 2000, Tarnocai et al., 2009). This carbon is not permanently sequestered but rather is present in soil as the balance of large fluxes both into and out of soils. The CO<sub>2</sub> flux from soils to the atmosphere is estimated at ~ 68 PgC/yr. GT per year, an enormous value even compared to the anthropogenic emission value of ~ 9 PgC/year (Raich and Schlesinger, 1992, Peters et al., 2012). Given the size of the soil carbon pool and associated flux, even small changes in the rate of soil organic matter decomposition could impact the forcing of the global climate system. Therefore, it is important to understand what mechanisms control the persistence, or lack thereof, of carbon in soils. This understanding is required in order to accurately predict changes in soil organic carbon (SOC) stocks in response to changes in climatic conditions like temperature and moisture or changes in direct anthropogenic impacts like land use or management practices. The ability to make such predictions is also important for developing strategies for climate impact mitigations like terrestrial carbon storage and biofuels production.

Of the potential mechanisms that control the persistence of organic matter in soils, association with minerals through sorption or precipitation reactions is thought to be one of the most important (Schmidt et al., 2011, Lehmann and Kleber, 2015). The importance of mineral organic associations (MOAs) and their capacity to contribute to the persistence of carbon in soil over long time scales has been demonstrated in the field and laboratory, and is consistent with results from new models. In the field, empirical studies involving natural pedogenic gradients have shown strong correlations between C stock or <sup>14</sup>C content with the mineral content, surface area, and mineral reactivity of soil

(Torn et al., 1997, Masiello et al., 2004, Mikutta et al., 2006, Lawrence et al., 2015, Porras et al., 2017). In the laboratory, incubation studies have demonstrated a decrease in bioavailability of carbon substrates when they are associated with minerals (Jones and Edwards, 1998, Mikutta et al., 2007, Kleber et al., 2015). Finally, model simulations that include simple sorption/desorption dynamics in the model reaction network lead to more realistic depth profiles of carbon concentration and  $^{14}\text{C}$  content (Riley et al., 2014, Dwivedi et al., 2017). These models assume that decomposition of labile compounds occurs only when those compounds are in the desorbed, aqueous phase, but this assumption has not been directly tested.

MOAs develop in soil through complex interactions between solid and solution phase organic constituents and the inorganic mineral matrix. Soil organic matter comprises a range of compounds with different elemental composition, size, and functional groups (Sutton and Sposito, 2005). Among this varied array, simple sugars, such as glucose, represent a class of abundant biomolecules. Glucose in particular is a central metabolite that is easily decomposed by multiple classes of organisms, making it an interesting test case for the impact of mineral associations on the fate of organic soil constituents. Like the various molecular assemblages which comprise soil organic matter, the inventory of soil minerals is diverse with a wide range of reactivities and capacities for stabilization of organic soil constituents. Iron (hydr)oxides are a class of soil minerals with wide distribution in soils and are present to at least some degree in virtually all soils, with concentrations that range between  $< 1$  and several hundred g/kg (Cornell and Schwertmann, 1996). Due to their low solubility, iron (hydr)oxide concentrations in soils tend to increase with increased weathering making them one of the most persistent soil mineral phases. Of the iron (hydr)oxides, goethite is the most common in soils, whereas ferrihydrite has the highest surface area and is generally considered to be the most reactive (Cornell and Schwertmann, 1996). Both are characterized by high reactive surface area compared to other soil minerals and have a demonstrated capacity to adsorb and stabilize organic compounds in terrestrial as well as aquatic environments (Tipping, 1981, Kaiser and Guggenberger, 2007, Kaiser et al., 2007, Eusterhues et al., 2008, Ghosh et al., 2009, Lalonde et al., 2012, Andrade et al., 2013, Hernes et al., 2013, Shimizu et al., 2013, Kleber et al., 2015). While natural specimens of goethite and ferrihydrite can contain trace metals like Al and other impurities that impact their geochemical properties, extensive investigations of iron oxide mineral structure and properties have made it possible to create synthetic versions of these minerals with key properties of structure and surface area similar to those found in soils (Cornell and Schwertmann, 1996, Schwertmann and Cornell, 2007b).

The mechanism of association between an organic molecule and a mineral depends on the specific chemical and physical characteristics of the mineral phase and the organic compound, as well as soil solution properties including pH and ionic strength. While some MOAs are formed via classic

sorption/desorption phenomena, many are a result of more complex surface phenomena such as surface complexation reactions, co-precipitation, and formation of multi-layer structures. Glucose can sorb to Fe (hydr)oxides via hydrogen bonding mechanisms (Olsson et al., 2011) or can associate via ill-defined co-precipitation processes (Eusterhues et al., 2011, Henneberry et al., 2012). Jagadamma et al. (2012) examined the adsorption of five well-defined organic compounds including glucose in soils from nine locations and three soil orders (Mollisols, Ultisols, and Alfisols) (Jagadamma et al., 2012). The Ultisol sorbed more glucose than did the other two soil orders, potentially because of their higher Fe (hydr)oxide and clay content although no statistically significant relationships were found. Mayes et al. (2012) examined DOC sorption behavior in 213 distinct soils, finding that DOC sorption capacity was positively correlated with Fe (hydr)oxide content and/or texture, highlighting the role of surface area and Fe (hydr)oxides in forming MOAs (Mayes et al., 2012). Furthermore, Vogel et al. (2014) showed that even when average bulk loadings are not particularly high, OM can be associated with surfaces in a clustered rather than layered manner and that new organic matter added to the system preferentially associates with existing organic patches suggesting the importance of organic-organic interactions along with organic-mineral interactions in controlling MOA behavior (Vogel et al., 2014).

Association with minerals via adsorption to or co-precipitation with metal (hydr)oxide phases or the formation of multi-layer OM-OM bonds with mineral stabilized organic compounds can significantly decrease the bioavailability of otherwise decomposable organic molecules (Kleber et al., 2015). Using a complex mixture of OM (forest floor extract) rather than a single compound, Mikutta et al. (2007) found a 50–90% decrease in the decomposition of organic matter over a 90-day period when sorbed to goethite (Mikutta et al., 2007). They also found that the linear association constant (K) for the OM-goethite mixture had a negative correlation with the fraction of organic matter mineralized, implying that the strength of association between the OM and the mineral affects decomposition behavior. Jones and Edwards (1998) observed that association with ferrihydrite significantly decreased decomposition of  $^{14}\text{C}$  labeled glucose and/or citrate in a model soil incubation (Jones and Edwards, 1998). A similar impact of mineral surface association was observed in bacterial culture in which pre-equilibration with ferrihydrite significantly decreased glucose decomposition (Jones and Edwards, 1998).

The ability of MOAs to stabilize organic carbon has also been invoked as an explanation for the frequently observed trend of decreasing  $^{14}\text{C}$  content with depth within a soil profile with the hypothesis being that lower OM to mineral ratios at depth means a larger fraction of MOA associated carbon and therefore greater stabilization of carbon at depth (Kogel-Knabner et al., 2008). Alternative hypotheses for the  $^{14}\text{C}$  depth trend exist including greater separation between substrates and decomposers, substrate limitation, and

nutrient supply (Rumpel and Kogel-Knabner, 2011). Though as mentioned above, the modeling work of Riley et al. (2014) showed that the sorption/desorption behavior could explain the observed trend. However, there has been little work directly examining the behavior of MOAs in deeper soils in order to directly address this observation (Riley et al., 2014).

In addition to understanding their impact on SOC dynamics throughout the soil profile, there is little known about how MOAs will respond to changes in environmental conditions, such as temperature and moisture variations. Because each class of MOA may have a different response to these factors, it would be ideal to take a systematic approach to understanding these dynamics. On the other hand, the vast complexity of MOAs in soil make it impractical to treat every type of MOA individually. In the work described here, we attempt to balance realism with tractability, focusing on the dynamics of MOAs formed between representative Fe (hydr)oxides (ferrihydrite and goethite) and glucose, a common soil molecule, as a representative of an easily decomposable, weakly sorbing organic species.

By using  $^{13}\text{C}$ -labeled glucose as opposed to a soil extract or other unlabeled compound, we are able to quantify the specific decomposition (mineralization to  $\text{CO}_2$ ) of the glucose-MOAs incubated in soil. The soils used in the incubations were collected as a function of depth and the incubations subjected to different temperature conditions. In this way, the current work is unique and potentially more relevant to field conditions than the studies cited above and others that explored the impact of mineral association on decomposition in incubations using soil inocula or other approaches aimed at quantifying the decomposition of the mineral associated carbon (Kaiser and Guggenberger, 2000, Kalbitz et al., 2005, Scheel et al., 2007, Schneider et al., 2010, Eusterhues et al., 2014). By using well-defined  $^{13}\text{C}$ -labeled MOAs, we were able to advance understanding of sorption/desorption behavior and its effect on the decomposability of a specific mineral-associated compound in the complex soil environment, with competing organic substrates and native mineral assemblages.

## 2. Material and methods

### 2.1. Fe (Hydr)oxide synthesis and characterization

The method of synthesis used in the present study was adapted from Schwertmann and Cornell, 2007c, Schwertmann and Cornell, 2007a. While the diversity of natural minerals is great, synthetic versions of these iron oxides are widely accepted to represent the major characteristics, e.g. crystal structure and surface area, of their natural counterparts. A detailed description of iron oxide mineral structures and their geochemical properties can be found in Cornell and Schwertmann (1996). Synthetic goethite and ferrihydrite mineral phases were prepared via titration of a 0.01 M Iron (III) nitrate solution to pH 7 with slow addition of 1 M sodium hydroxide. Once the end point was attained, the mixture was allowed to equilibrate for 1 h with base added dropwise until the solution pH

stabilized. Synthetic goethite was produced by aging of the Fe hydroxide precipitate for 11 days at 80 °C which drives structural re-ordering of ferrihydrite to the well-crystalline goethite phase. Post-synthesis, Fe-(hydr)oxide phases were re-suspended in Nanopure reagent grade water (18.2 MΩ-cm), rinsed once to remove residual sodium ions, and mixed with ultrapure silica sand (Iota 6, Unimin Corp., USA). The synthetic ferrihydrite- and goethite-quartz sand slurries were mixed in a stream of air until all water was evaporated. The identity and purity of the synthetic ferrihydrite and goethite phases were confirmed via powder X-ray diffraction using a PANalytic X'Pert Pro X-ray diffractometer with Co K $\alpha$  radiation source (PANalytical, Inc., the Netherlands). The BET measured surface areas for ferrihydrite and goethite of 42 and 205 m<sup>2</sup>/g, respectively were also shown to be within the expected range for each mineral type (Cornell and Schwertmann, 1996). In addition, mass of Fe per gram of goethite or ferrihydrite coated sand was determined via a 6 M HCl extraction. Samples were spiked with 1 ppm scandium internal standard and analyzed in triplicate using an iCap 6300 DUO ICP-OES (Thermo Scientific, USA).

## 2.2. Determination of adsorption maxima and preparation of <sup>13</sup>C labeled Fe organic associations

Adsorption experiments with glucose and synthetic Fe (hydr)oxide coated sand were carried out at a sorbent to sorbate ratio of 1:2 over a concentration range of 1 to 50 mM in batch reactors at 25 °C for 12 h in 0.5 M NaCl background electrolyte solution in the dark. A solution pH of 6.5 was selected because it is within the range of pH (5–7) of the soils from our experimental site. Best possible effort was made to maintain sterile conditions during sample preparation through the use of autoclaved glassware, solutions, and solids. Equilibrium glucose concentrations were determined via HPLC (Agilent, USA) and the amount adsorbed by the solid Fe (hydr)oxide was computed by difference from the initial added concentration. Calculated adsorption maxima were utilized to prepare synthetic glucose Fe-(hydr)oxide associations near 100% saturation of the mineral surface. Resulting sorption data were fit to three common numeric sorption isotherms (Freundlich, Langmuir, and Linear) using a least square fitting routine in excel. In the case of the Langmuir parameters, the linearized form of the relationship was used in the fitting procedure ( $C/q = 1/kQ_{\max} + C/Q_{\max}$ ; where C is glucose concentration in mol L<sup>-1</sup>, q is surface excess in mol g<sup>-1</sup>; k is the Langmuir binding constant, and Q<sub>max</sub> is the Langmuir maximum sorption capacity).

To prepare synthetic MOAs for the incubations, sterile 9.9 Atom % <sup>13</sup>C-glucose solution (Cambridge Isotope Laboratories, USA) was reacted with Fe-(hydr)oxide coated sands for 12 h in the dark. Before incorporation into the soil for bioavailability tests, the synthetic MOAs were subjected to a desorption test, which constituted rinsing the MOA material in a glucose free solution and separating the wash supernatant from the solid via

centrifugal filtration. The glucose concentration in solution post-rinse was subsequently determined via HPLC.

### 2.3. Soil incubations

Incubations were conducted using bulk soils collected from three depths (10–20, 50–60, and 80–90 cm) at the Blodgett Forest Research Station, Georgetown, CA. The soils are moderately acidic (~ pH 6.0) sandy, mixed, mesic Ultic Haploxeralfs. Soils were picked free of visible roots and transferred to 160 mL serum bottles. Sterile Nanopure (18.2 MΩ-cm) was added such that total soil water content was equivalent to 25% Volumetric Moisture Content (VMC). Experimental treatments for each depth are as follows: <sup>13</sup>C-glucose-ferrihydrite (<sup>13</sup>C Fh) coated sand added to native soil (n = 3); <sup>13</sup>C-glucose-goethite (<sup>13</sup>C Gt) coated sand added to native soil (n = 3); native soil with nothing added (NA) control with no glucose or mineral adduct (n = 3); ferrihydrite coated sand disturbance (Fh. Control) control added to native soil without glucose (n = 3); and <sup>13</sup>C-labeled non-mineral associated glucose (<sup>13</sup>C glucose) control added directly to the soil (n = 3). The amount of <sup>13</sup>C-labeled glucose added to the soil equaled 5% of the mineral-associated C as defined by density fractionation for each depth interval. All treatments were incubated at 25 °C and headspace CO<sub>2</sub> was sampled at 0, 1, 24, and 48 h for 0–10 cm and at 0, 24, 48, and 72 h for 50–60 and 80–90 cm. After ~ 80 days (1896 h), the headspace CO<sub>2</sub> was re-sampled and the temperature of the incubations was increased to 30 °C in order to assess the temperature sensitivity of both the native carbon and the mineral associated <sup>13</sup>C-labeled glucose. Headspace CO<sub>2</sub> was again measured at 0, 1, 24, and 48 h for the 10–20 cm samples, and 0, 24, 48, and 72 h for the 50–60 and 80–90 cm samples. Sample [CO<sub>2</sub>]<sub>ppmv</sub> was determined by gas chromatography (Shimadzu, USA). The δ<sup>13</sup>C value of the headspace CO<sub>2</sub> was determined via syringe injection using a cavity ring down spectrometer (CRDS) isotopic CO<sub>2</sub> analyzer with small sample injection module (SSIM; Picarro, USA). CO<sub>2</sub> concentrations and δ<sup>13</sup>C values measured over the four time points were used to calculate flux rates and quantify the <sup>13</sup>C-labeled glucose that was bioaccessible to soil microbes. Initial, t = 0, CO<sub>2</sub> headspace values were subtracted from subsequent values in order to remove any impact from different concentrations of room air present in the headspace. In order to compare to other results taken at 72 h, the 30 °C samples for which the longest measured time point was 48 h, were linearly extrapolated for an additional 24 h using the average CO<sub>2</sub> flux measured from the first 48 h.

The total amount of carbon respired or mineralized (C<sub>lost</sub>) during the incubation was calculated using the following equation:

$$C_{lost} = C_f - C_i T$$

where the amount of carbon at the start of the incubation (C<sub>i</sub>), either in the jar headspace or total sample was subtracted from the amount of carbon at end of the incubation (C<sub>f</sub>), either in the headspace or solid sample, divided



by the duration of the incubation. For the headspace samples, the amount of carbon removed during time course sampling was taken into account and added to the  $C_f$  value. For the cumulative carbon respired over time, the amount of carbon in the jar headspace (taking the amount of carbon removed to sample into account) for each time point was divided by the mass of the soil being incubated. The proportion of respired carbon coming from either native soil ( $f_s$ ) or added glucose ( $f_g$ ) was calculated using the following set of equations:

$$1 = f_s + f_g$$

$$C_{13\text{sample}} = f_n * C_{13n} + f_g * C_{13g}$$

where the proportion of native soil carbon ( $f_n$ ) and glucose carbon ( $f_g$ ) were unknowns and the  $^{13}\text{C}_{\text{sample}}$  was known from either the sampled headspace  $\text{CO}_2$  or the solid soil sample, the  $^{13}\text{C}_g$  was known (9.9 atom%), and the  $^{13}\text{C}_n$  was known from control samples (either headspace or soil) to which no glucose had been added. These proportions were then multiplied by the amount of carbon respired or mineralized to get the amount of native carbon or glucose carbon respired or mineralized. Reported errors for final values are propagated through the calculation from the original uncertainty in the measurement values as determined by accuracy of calibration and scatter from the replicate data points. Reported standard errors associated with rates derived from the linear regressions with time are calculated from standard regression analysis using all the individual replicate values.

#### 2.4. Solid phase isotope-ratio mass spectrometry (IRMS) data

Following the 25 °C incubation at 1896 h, stable isotopic analysis and determination of carbon content of  $^{13}\text{C}$ -labeled glucose treated soils and natural abundance controls was performed via solid phase combustion using a Thermo Delta V Plus isotope ratio mass spectrometer interfaced to a Costech ECS 4010 CHNSO analyzer at the Center for Isotope Geochemistry at Lawrence Berkeley National Laboratory. Prior to analysis, the soils were oven dried at 50 °C until no further mass loss was observed and homogenized using a SPEX 8000 M mixer mill. Measured  $\delta^{13}\text{C}$  and C concentration values were used to quantify the proportion of bioaccessible mineral associated  $^{13}\text{C}$ -labeled glucose in our soils. Percent decomposed was calculated by dividing the total of the remaining  $^{13}\text{C}$  glucose post-incubation by the sum of the respired glucose and the glucose remaining in the samples post-incubation.

### 3. Results and discussion

#### 3.1. Sorption isotherms

To explore the nature of glucose-mineral interaction and to ensure the desired, consistent loading of glucose for the incubations, we determined glucose sorption isotherms on ferrihydrite and goethite coated sands as a function of equilibrium glucose concentrations up to a maximum of ~ 50 mM

(Fig. 1). The surface excess on ferrihydrite-sand increased rapidly with equilibrium glucose concentration up to an apparent plateau around  $\sim 35\text{--}45 \text{ mmol glucose g}^{-1} \text{ Fe}$  implying potential saturation of available sorption capacity. On the goethite-sand, the shape of the sorption isotherm takes on a more sigmoidal-type shape implying a changing affinity for the surface with increased surface loadings and potentially sorbate-sorbate interactions (Sposito, 2008). A similar sigmoidal-type curve was observed by Feng et al. (2015) for natural organic matter (NOM) on goethite at pH 6 which they interpreted as indicative of surface precipitation/condensation/coagulation of the absorbing organic matter emphasizing the importance of interactions on the surface beyond classic surface complexation or ion exchange. The data in Fig. 1 were fit to three commonly used numeric absorption descriptions, Langmuir, Linear, and Freundlich. (The specific fitting constants, associated errors, and comparison to some previous work are available in the Supplemental material.) The ferrihydrite data were fit relatively well by all three line shapes, whereas the goethite data were only fit well by the Linear, and Freundlich with very poor fits to the Langmuir. The poor fit to the Langmuir curve of the goethite data once again emphasizes the likelihood of non-classical sorption behavior of the glucose.

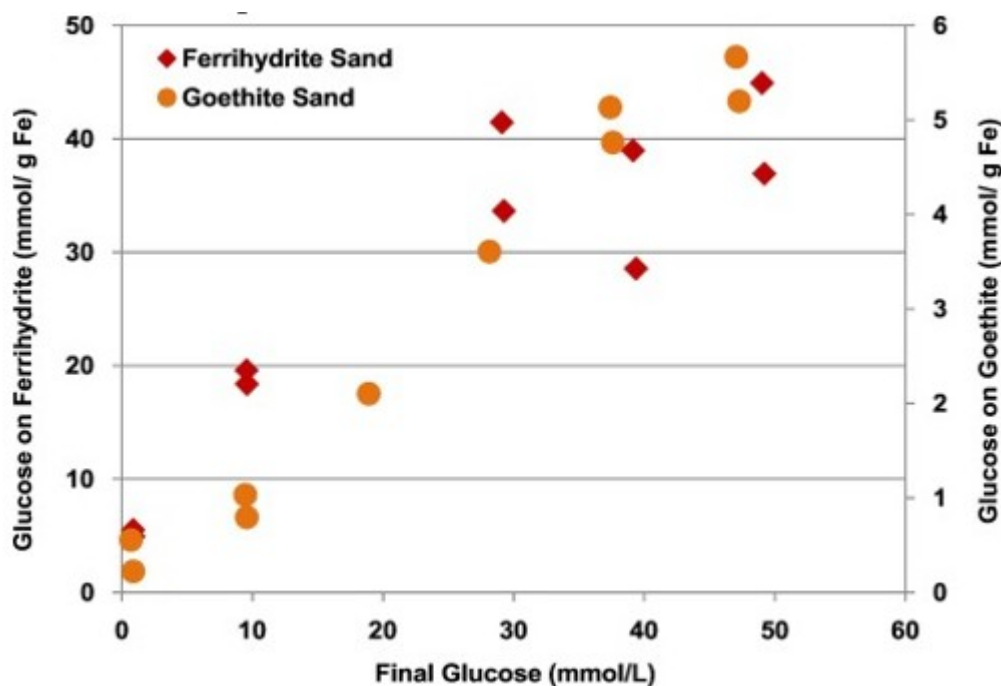


Fig. 1. Surface excess of glucose on ferrihydrite and goethite coated sands as a function of final glucose concentration.

The synthetic MOAs ( $^{13}\text{C}$ -labeled ferrihydrite and  $^{13}\text{C}$ -labeled goethite;  $^{13}\text{C}$  Fh and  $^{13}\text{C}$  Gt respectively) were subjected to a single Nanopure rinse to remove interstitial (non-sorbed) glucose prior to being used in the incubation experiment. The glucose that desorbed during the rinsing procedure was quantified via HPLC for both  $^{13}\text{C}$  Fh and  $^{13}\text{C}$  Gt. The  $^{13}\text{C}$  Fh and  $^{13}\text{C}$  Gt released  $23 \pm 5\%$  and  $48 \pm 40\%$  of maximum surface-associated glucose,

respectively; the remaining loading level placed each of the MOAs at the steepest, or greatest affinity, region of the sorption isotherm in Fig. 1. In other words, the incubated MOAs were not at maximum potential surface loading, but at a position on the isotherm where glucose exhibits a high affinity for both surfaces. Thus, the most easily desorbed glucose had been released and the remaining surface-bound material was at least somewhat resistant to further desorption.

### 3.2. Total C respiration

The respiration rate per gram soil in nothing added (NA) control soils to which no MOAs or free glucose were added was much higher in the 10–20 cm depth as compared to the deeper soils (Fig. 2). The linear respiration rates for the three depth increments, 10–20 cm, 50–60 cm, 80–90 cm, over the first 96 h were  $0.27 \pm 0.01$ ,  $0.017 \pm 0.001$ , and  $0.018 \pm 0.003 \mu\text{g C g soil}^{-1} \text{ h}^{-1}$ , respectively. The respiration rates for all three depths were similar when normalized by soil C content (Fig. 2b), suggesting that decomposition of organic carbon in the deeper soils, relative to the shallow soil, was not limited by lower abundance of decomposers or moisture or oxygen availability (the incubated soils had undergone physical mixing and moisture addition) under these laboratory conditions. The 50–60 and 80–90 cm depths had a greater initial rate of normalized carbon respiration as can be seen by the differences in the 24 h time points in Fig. 1A and B. From 24 h on in time the respiration rate is sustained in a nearly linear way until the final time point shown at 96 h. The relatively higher initial rate in the deeper soil could be due to disturbing the soil structure during field collection and handling in the laboratory (Salome et al., 2010). The relative similarity of normalized rates appears to have continued for an extended period: when the incubations were resampled at  $\sim 80$  days the headspace  $\text{CO}_2$  concentrations were and  $2800 \pm 200$  (10–20 cm),  $2200 \pm 200$  (50–60 cm),  $2000 \pm 300$  (80–90 cm),  $\mu\text{g C g}^{-1}$  native soil carbon.

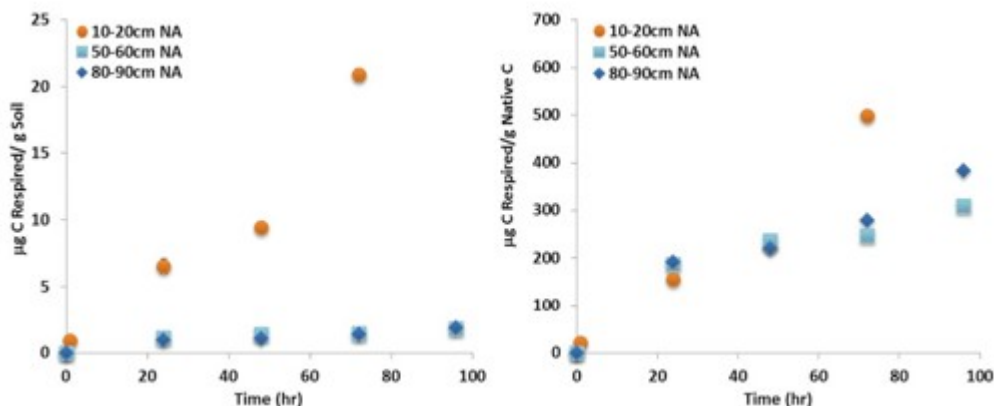


Fig. 2. Cumulative C respired from native soil (no amendment added) for three depths A) C respired  $\text{g}^{-1}$  soil. B) C respired  $\text{g}^{-1}$  soil C. Standard error bars shown but are smaller than symbols.

The respiration rate of total carbon, native carbon, and added glucose from treatments to which free  $^{13}\text{C}$ -glucose was added are shown in Fig. 3.

Compared to the natural abundance controls (Fig. 2) respiration increased at all depths in the  $^{13}\text{C}$ -glucose addition treatments (Fig. 3). The linear respiration rates for the native carbon to which  $^{13}\text{C}$ -glucose had been added were  $0.31 \pm 0.02$ ,  $0.089 \pm 0.004$ , and  $0.045 \pm 0.001 \mu\text{g C g soil}^{-1} \text{ h}^{-1}$ , at 10–20 cm, 50–60 cm and 80–90 cm, respectively. These rates were  $\sim 120\%$ ,  $\sim 520\%$ ,  $\sim 250\%$  greater than those in the respective natural abundance controls. The increase in native carbon respiration after the glucose addition, as well as the rapid respiration of the added glucose itself, implies a carbon- or energy-limited state for the deeper soils that is alleviated by the addition of the glucose, similar to the response caused by the addition of cellulose to deep soils in (Fontaine et al., 2007). The respiration rate at 50–60 cm increased the most, suggesting the mid-depth is the most substrate-limited of the three depths, followed by 80–90 cm. No major limitation to glucose mineralization was apparent as evidenced by the fact that at  $\sim 80$  days,  $78 \pm 8\%$  of the added glucose was respired in 10–20 cm and  $169 \pm 5\%$  and  $125 \pm 8\%$  for both the 50–60 cm, and 80–90 cm soils respectively (the two member mixing model can give over 100% due to the small uncertainty in the measurements). Over the full 80 days, the specific respiration rate of native carbon in the 50–60 cm from the glucose-amended soils continued to be the largest, further supporting the conclusion that this depth is the most substrate limited of the three.

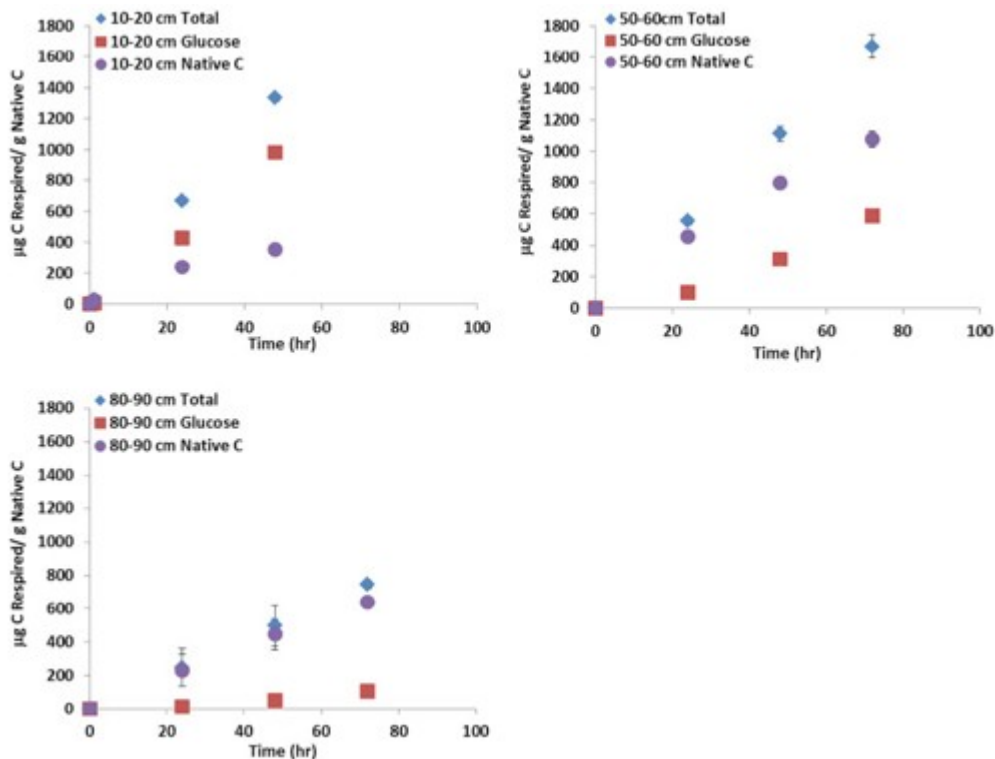


Fig. 3. Cumulative C respired from the soil to which free  $^{13}\text{C}$ -glucose had been added, as glucose C, native C, and total C respired. One panel per soil depth. Standard error bars shown but smaller than symbol.

### 3.3. $^{13}\text{C}$ respiration

The total respiration from the treatments in which the synthetic MOAs of  $^{13}\text{C}$ -labeled ferrihydrite and  $^{13}\text{C}$ -labeled Goethite ( $^{13}\text{C}$  Fh and  $^{13}\text{C}$  Gt respectively) are compared to the nothing added (NA) controls in Fig. 4. In spite of the same amount of total glucose being added as in the free glucose controls, Fig. 3, the total respiration in the mineral treatments is similar to that in the NA controls indicating that the bioavailability of the glucose in the MOAs was dramatically decreased compared to that of free glucose. Specifically, Table 1 shows the results of the calculated glucose bioavailability—or fraction of added glucose that was respired—in two different ways: (1) the amount of respired glucose at 72 h or 80 days divided by the mass of glucose added and (2) the amount of respired glucose at 72 h or 80 days divided by sum of the respired glucose and the  $^{13}\text{C}$  label recovered in soils at  $\sim 80$  days as determined by IRMS. Calculated in the first way, the fraction of mineral-associated  $^{13}\text{C}$ -glucose decomposed in the first 72 h was 0.01–0.15% and at 80 days 0.07 to 0.2%, Table 1. Calculated the second way, the percentage of decomposed mineral-associated  $^{13}\text{C}$ -glucose at 80 days were about an order of magnitude larger, although still 3% or less, Table 1. The  $^{13}\text{C}$ -recovery (IRMS) method confirms that the target amount of  $^{13}\text{C}$  was added to the soil in the MOA, and that the very low respired- $^{13}\text{C}$  values were not an experimental artifact. The high standard errors reported in Table 1 derive from scatter in the IRMS data; the scatter in the respiration data was minimal. Thus, we refer to the results of the first method in the following.

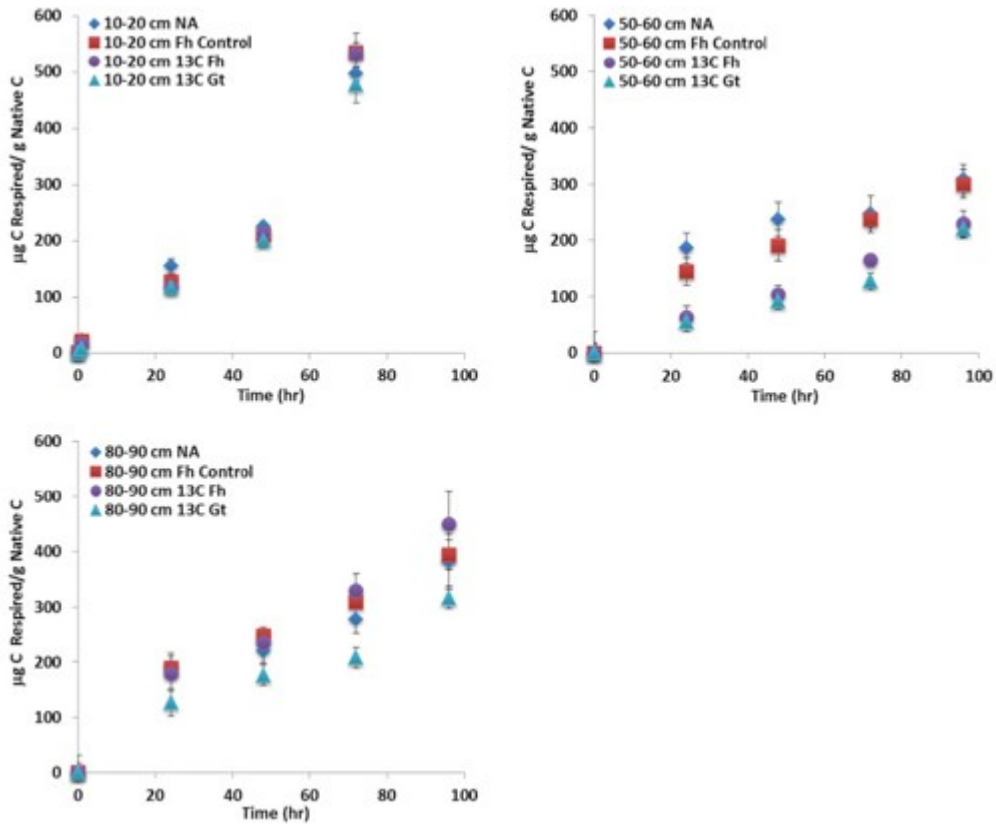


Fig. 4. Cumulative respiration per gram soil C in unamended soils and all soils to which minerals were added. A) 10–20 cm, B) 50–60 cm, C) 80–90 cm. Standard error bars shown. Data plotted are total respiration but are equivalent to native C respiration due to the extremely low contribution of  $^{13}\text{C}$  from MOA treatments, see Table 1. Labels: Nothing added (NA); Glucose free Ferrihydrite (Fh. Control)  $^{13}\text{C}$ -labeled ferrihydrite (13C Fh);  $^{13}\text{C}$ -labeled Goethite (13C Gt).

Table 1. The amount of  $^{13}\text{C}$  glucose decomposed, as a percent of the amount added or amount recovered post incubation, at 72 h and 80 days and when warmed by 10 °C. The amount of  $^{13}\text{C}$  added in MOA form was calculated from the mass and  $\delta^{13}\text{C}$  value of the MOA added.

Decomposed glucose (% of added glucose) at 72 h	Decomposed glucose (% of added glucose) at 80 days	Decomposed glucose (% of recovered $^{13}\text{C}$ label) at 72 h	Decomposed glucose (% of recovered $^{13}\text{C}$ label) at 80 days	+ 5 °C for 72 h Decomposed glucose (% of added glucose) applied at 80 days
---	--	---	--	--

10–20 cm

	<b>Decomposed glucose (% of added glucose) at 72 h</b>	<b>Decomposed glucose (% of added glucose) at 80 days</b>	<b>Decomposed glucose (% of recovered <sup>13</sup>C label) at 72 h</b>	<b>Decomposed glucose (% of recovered <sup>13</sup>C label) at 80 days</b>	<b>+ 5 °C for 72 h Decomposed glucose (% of added glucose) applied at 80 days</b>
<b><sup>13</sup>C “free” glucose</b>	80 (1) <sup>b</sup>	78 (8)	-	-	-
<b><sup>13</sup>C Fh MOA</b>	0.16 (1)	0.18 (2)	3 (1)	3 (1)	0.056 (6)
<b><sup>13</sup>C Gt MOA</b>	0.09 (3)	0.07 (4)	1.1 (4)	0.7 (4)	0.05 (2)
50-60 cm					
<b><sup>13</sup>C “free” glucose</b>	19 (1)	169 (5)	-	-	-
<b><sup>13</sup>C Fh MOA</b>	0.017 (2)	0.16 (1)	0.18 (2)	2 (1)	0.14 (1)
<b><sup>13</sup>C Gt MOA</b>	0.011 (1)	0.072 (5)	0.503 <sup>a</sup>	3.0 <sup>a</sup>	0.051 (5)
80-90 cm					
<b><sup>13</sup>C “free”</b>	8.5 (9)	125 (8)	-	-	-

	Decomposed glucose (% of added glucose) at 72 h	Decomposed glucose (% of added glucose) at 80 days	Decomposed glucose (% of recovered <sup>13</sup> C label) at 72 h	Decomposed glucose (% of recovered <sup>13</sup> C label) at 80 days	+ 5 °C for 72 h Decomposed glucose (% of added glucose) applied at 80 days
<b>"</b>					
<b>glucose</b>					
<b><sup>13</sup>C</b>					
<b>Fh</b>	0.027 (2)	0.08 (1)	0.4 (2)	1.1 (5)	0.070 (5)
<b>MOA</b>					
<b><sup>13</sup>C</b>					
<b>Gt</b>	0.043 (9)	0.2 (2)	-	-	0.1 (1)
<b>MOA</b>					

( ) show standard error in last reported digit.

a Single IRMS measurement.

b 72 h value extrapolated from 0 to 48 h data for comparison purposes.

In contrast to the MOA treatments the added free glucose was nearly mineralized completely, with 80% decomposed within the initial 72 h experimental period in the 10–20 cm implying very rapid microbial utilization. The fact that even after 80 days only 78% of the free glucose is respired could simply be due to lack of sufficient time for decomposition, some degree of stabilization of added glucose, the level of certainty in the method, or that the <sup>13</sup>C not measured as respired CO<sub>2</sub> could have been incorporated into microbial biomass. The 80% fraction is in agreement with reported carbon use efficiencies for soil microbial communities (Geyer et al., 2016). When the percent utilization values from the MOA treatments are compared to the associated utilization of the free glucose addition, it is possible to calculate that association with the mineral surface results in a decrease in bioavailability of > 99.5% across all depths.

While it was expected that the glucose associated with the MOA would have reduced bioavailability, the extremely low bioavailability of the carbon in the MOA is striking and emphasizes the impact that mineral association can have on this otherwise readily decomposable substrate. The higher relative



bioavailability of the MOA glucose in the near-surface depth increment could be due to the presence of greater concentrations of native organic carbon. This potentially greater abundance of organic ligands in native organic matter within the near-surface soils could facilitate to some degree desorption of glucose from mineral surfaces due to competitive interaction (Sposito, 2008). Alternatively, the microbial community could have greater access to bioenergetic resources enabling access to otherwise unavailable mineral-associated carbon (Fontaine et al., 2007).

The > 99.5% decrease in glucose respiration as a result of association with goethite or ferrihydrite is the most dramatic result in the current work, but there are several additional findings in the following discussion. While the estimated surface loadings of the synthetic MOAs used in the study exceeded the hypothesized maximum surface loadings of  $\sim 1 \text{ mg C/m}^2$  (Feng et al., 2013, Feng et al., 2014), the mineral-associated organic material was highly resistant to decomposition, showing the importance of mineral-organic interactions beyond classic sorption-desorption behavior. Sorption results from both Feng et al. (2015) and our study suggest that the MOAs in this system were likely in a region of surface precipitation/condensation/coagulation rather than classic monolayer sorption (Vogel et al., 2014, Feng et al., 2015). The difference in conceptual models, between monolayer surface association and complex three-dimensional surface structures that are nonetheless resistant to decomposition, has implications for how MOA formation and behavior are understood and modeled. If a simple molecule like glucose is capable of complex intermolecular behavior on Fe (hydr)oxide surfaces with dramatic impact on rates of decomposition, it is likely to be even more important for larger organic molecules with their greater degrees of conformational freedom and more diverse functional group composition.

Table 1 shows the very small change in the cumulative amount of MOA glucose decomposed between 72 h and 80 days. In fact, in three of the six treatments, the total amount respired did not increase significantly. A simple explanation of this result would be that much of the apparent bioavailability of the glucose in the MOAs is a result of mineralization of the small amount of interstitial (non-mineral bound) glucose added with the MOA at the beginning of the experiment or of a small amount of initial desorption followed by virtually no release of further material. Both of these explanations would imply that the extremely low bioavailability of MOA-glucose reported above may still be an under estimation. However, under field soil conditions moisture conditions would vary and this variation might repeatedly drive release of additional carbon from the mineral surface and make it available for mineralization.

#### 3.4. Impact of carbon free mineral surfaces

Also shown in Fig. 4 are the results from the treatment in which  $^{13}\text{C}$  glucose free ferrihydrite was added to the soil (Fh Control). For the soils from 10 to

20 cm there were no measurable differences between the mineral treatments and the natural abundance controls. However, for the 50–60 cm depth, the respiration of native C in all three mineral treatments ( $^{13}\text{C}$  Fh,  $^{13}\text{C}$  Gt, and Fh control) was lower than that in the natural abundance controls during the initial  $\sim 100$  h time period; the difference was statistically significant for the  $^{13}\text{C}$  Fh and  $^{13}\text{C}$  Gt treatments (Single factor ANOVA with post-hoc *t*-test, Holm–Bonferroni adjusted  $p < 0.1$ ). In the 80–90 cm depth, respiration of native C from the  $^{13}\text{C}$  Gt treatment was lower than from the other treatments, but the difference not statistically significant. The observed decrease in cumulative respiration of native C in the 50–60 cm depth due to mineral addition ( $^{13}\text{C}$  Fh and  $^{13}\text{C}$  Gt) could result from the accompanying addition of carbon-free mineral-surface sites to the system thereby facilitating sorption of otherwise decomposable substrates and rendering them inaccessible to microbes. The fact that this effect was greatest in the 50–60 cm depth is consistent with the observation that this depth was the most substrate limited of the three depths, and therefore potentially the most sensitive to added mineral surface area further restricting substrate availability.

If the added mineral surface area from the  $^{13}\text{C}$  Fh and  $^{13}\text{C}$  Gt MOA decreased substrate availability in the 50–60 cm depth, it is somewhat surprising that the Fh disturbance control did not show a significant impact on total respiration given that this mineral should have all of its' surface binding sites available. This apparent contradiction could be due to a small difference in experimental protocol between the treatments: the MOAs were added to the soil as a wet paste, while the synthetic mineral in the Fh control was added to the soil dry. The water film surrounding the MOAs when added to the soil could have facilitated sorption of native carbon in a way not observed in the dry samples, even though the sample treatments were all adjusted to the same bulk soil moisture after addition of the minerals. This explanation would suggest an important role for moisture in controlling the impact of mineral surfaces on substrate availability.

Another interesting result is that non-mineral associated glucose added directly to deeper soils does not appear to have sorbed to native mineral surfaces rapidly enough to prevent its decomposition. In spite of the obvious analytical error associated with  $> 100\%$  decomposition values calculated for  $^{13}\text{C}$  glucose controls in the 50–60 cm and 80–90 cm samples (Table 1), it is significant that even in the high mineral-density deeper horizons, the added glucose was completely decomposed because it would be expected that some fraction of the free glucose would have become associated with native minerals. The fact that synthetic MOAs were formed with fresh, carbon-free mineral surfaces whereas the free  $^{13}\text{C}$ -glucose was added directly to the bulk soil where the mineral surfaces are likely already coated with different types of organic and inorganic absorbents may have been a factor limiting sorption of the glucose solution with native soil minerals, but would not be consistent with previous results that suggest existing carbon on

mineral can facilitate further association (Vogel et al., 2014). Alternatively, it may again emphasize the importance of moisture for facilitating the transport of added OM to mineral surfaces. The synthetic MOAs were made in full aqueous suspensions, facilitating the association of the glucose with the synthetic mineral and achievement of a low energy configuration, whereas in the free glucose incubation treatments the glucose was added to soils at ~ 25% VMC, which while fairly moist and well mixed afterwards, is not likely to facilitate the same degree of glucose mobility as an aqueous suspension as seen in the case of Jones and Edwards (1998). This observation along with the discussion above of why the ferrihydrite disturbance control showed less of an impact than the MOA treatments emphasizes the importance of the formation conditions, particularly moisture, on the impact of MOAs on carbon decomposability.

### 3.5. Impact of 5 °C temperature increase

Because the temperature sensitivity of different pools of soil organic matter is of particular interest in understanding how soil organic matter stocks might respond to a changing climate, we examined the impact of increased temperature on respiration of MOA organic matter. Specifically, after ~ 80 days, the temperature of the incubations was increased from 25 °C to 30 °C to test the impact of elevated temperature on the decomposition of the MOA glucose. The increase in total CO<sub>2</sub> respiration measured over 72 h at 30 °C in the NA treatments at all depths was larger than that measured in the original 72 h of the incubation at 25 °C, specifically ~ 3 ×, for 10–20 cm, ~ 6 × for 50–60 cm, and ~ 8 × for 80–90 (data not shown). The fraction of MOA carbon decomposed at higher temperature is shown in Table 1. In the 10–20 cm samples, the fraction of mineral-associated carbon decomposed at 30 °C is less as compared to 25 °C. At the other depths, the mineral-associated fraction decomposed increases, but with the exception of the <sup>13</sup>C Fh MOA the increase in respiration is less for the MOA carbon than for the corresponding native carbon. With no consistent pattern between depths and between types of MOA, it would be inappropriate to infer too much from these results. However the results suggest less temperature sensitivity of MOA carbon respiration compared to bulk native carbon respiration.

## 4. Conclusions

Association with Fe (hydr)oxide minerals dramatically decreased decomposition of added glucose, generally by over 99.5% relative to free-glucose mineralization, which was almost completely decomposable in all depths. Thus, mineral association has the potential to decrease the decomposition of even highly decomposable substrates. Given the high carbon surface loadings of the minerals in this study, this result also emphasizes the importance of more complex surface-association mechanisms (beyond classic sorption/desorption) on carbon stability on mineral surfaces. Although total respiration decreased with depth as

expected, when respiration rates were normalized by carbon content they were similar between the three depths. We found that the temperature sensitivity of native-carbon respiration was greatest in the deepest soils and respiration of mineral-associated carbon was less sensitive to increased temperature than was native carbon. Additional results of the study include the potential importance that carbon free mineral surfaces can play in influencing carbon respiration in substrate-constrained soils like those from the 50–60 cm depth and suggest the importance of moisture on the formation of MOAs and their impacts in the soil environment. While the ideal moisture conditions for MOA formation likely varies by organic matter and mineral type, it seems that strong MOAs may be more likely to form in high moisture conditions and in the presence of fresh mineral surfaces.

Looking at the importance of mineral association for stabilizing carbon in the larger context of climate change and land use change there are several interesting implications of the current results. The impact of increased temperature on the stability of soil carbon is of particular interest, and the current results, while preliminary, showing that MOA carbon is less temperature sensitive than the native SOM taken as a whole implies that mineral associated carbon may not represent a major positive climate feedback under increased temperature conditions. Beyond temperature, changes in moisture are another major potential climate change impact, and while we didn't address it directly in this work, the results suggest strongly that moisture conditions could be very important in the formation of MOAs. In addition, if moisture changes impact soil redox conditions thereby either promoting or retarding reductive dissolution of redox active minerals like iron (hydr)oxides this could in turn impact the release or update of the carbon. Beyond the physical transformations induced by environmental factors such as temperature and moisture, the response of the plant community to climate change and its coupling with the soil is likely to be a major factor in the fate of MOA carbon. Conditions, either natural or managed, that lead to deeper root growth and increased root exudation in low carbon, high mineral environments might lead to significant increases in the stock of MOA carbon either by coating organic free mineral surfaces or by enhancing primary weathering reactions which lead to fresh mineral production (Lynch and Wojciechowski, 2015). However, root exudation in the presence of existing MOAs might have the opposite impact through the dissolution of existing MOAs and the release of the associated carbon (Keiluweit et al., 2015). Finally, there is the question of direct anthropogenic intervention to increase the soil carbon sink. The fact that adding organic free mineral surfaces decreased the rate of respiration implies that direct addition of mineral surfaces perhaps from clean mining or industrial waste materials could potentially increase soil carbon storage, although it would need to be target to those soils where it would make the most impact. As seen in the current study, adding mineral surface area only made a significant impact in soils from the intermediate depths of the profile (50–

60 cm), presumably due to the specific ratio of organic matter to availability mineral surfaces. This in turn implies that understanding the total capacity of mineral surfaces to stabilize carbon relative to organic inputs is a key question for estimating the potential carbon storage benefit available through geo-engineering interventions like the ones above.

#### Acknowledgement

The authors thank Luca Corno and Gabriella Papa of the Joint Bioenergy Institute (JBEI) for HPLC access and assistance. We are also grateful to U.C. Berkeley undergraduate lab assistant Dafne Valdez for invaluable help with GC and C stable isotopic analysis of gas phase samples. This work was supported as part of the Terrestrial Ecosystem Science Program by the Director, Office of Science, Office of Biological and Environmental Research, of the U.S. Department of Energy under Contract no. DE-AC02-05CH11231.

#### References

Andrade et al., 2013

F.V. Andrade, E.d.S. Mendonca, I.R. da Silva **Organic acid adsorption and mineralization in OXISOLS with different textures**

Revista Brasileira De Ciencia Do Solo, 37 (2013), pp. 976-985

Cornell and Schwertmann, 1996

R.M. Cornell, U. Schwertmann **The Iron Oxides**

VCH-Verlagsgesellschaft, Weinheim (1996)

Dwivedi et al., 2017

D. Dwivedi, W.J. Riley, M.S. Torn, N. Spycher, F. Maggi, J.Y. Tang **Mineral properties, microbes, transport, and plant-input profiles control vertical distribution and age of soil carbon stocks**

Soil Biol. Biochem., 107 (2017), pp. 244-259

Eusterhues et al., 2008

K. Eusterhues, F.E. Wagner, W. Haeusler, M. Hanzlik, H. Knicker, K.U. Totsche, I. Koegel-Knabner, U. Schwertmann **Characterization of ferrihydrite-soil organic matter coprecipitates by X-ray diffraction and Mossbauer spectroscopy**

Environ. Sci. Technol., 42 (2008), pp. 7891-7897

Eusterhues et al., 2011

K. Eusterhues, T. Rennert, H. Knicker, I. Kogel-Knabner, K.U. Totsche, U. Schwertmann **Fractionation of organic matter due to reaction with ferrihydrite: coprecipitation versus adsorption**

Environ. Sci. Technol., 45 (2011), pp. 527-533

Eusterhues et al., 2014

K. Eusterhues, J. Neidhardt, A. Hadrich, K. Kusel, K.U. Totsche **Biodegradation of ferrihydrite-associated organic matter**

Biogeochemistry, 119 (2014), pp. 45-50

Feng et al., 2013

W.T. Feng, A.F. Plante, J. Six **Improving estimates of maximal organic carbon stabilization by fine soil particles**

Biogeochemistry, 112 (2013), pp. 81-93

Feng et al., 2014

W.T. Feng, A.F. Plante, A.K. Aufdenkampe, J. Six **Soil organic matter stability in organo-mineral complexes as a function of increasing C loading**

Soil Biol. Biochem., 69 (2014), pp. 398-405

Feng et al., 2015

W.T. Feng, J. Klaminder, J.F. Boily **Thermal stability of goethite-bound natural organic matter is impacted by carbon loading**

J. Phys. Chem. A, 119 (2015), pp. 12790-12796

Fontaine et al., 2007

S. Fontaine, S. Barot, P. Barre, N. Bdioui, B. Mary, C. Rumpel **Stability of organic carbon in deep soil layers controlled by fresh carbon supply**

Nature, 450 (2007), pp. 277-280

Geyer et al., 2016

K.M. Geyer, E. Kyker-Snowman, A.S. Grandy, S.D. Frey **Microbial carbon use efficiency: accounting for population, community, and ecosystem-scale controls over the fate of metabolized organic matter**

Biogeochemistry, 127 (2016), pp. 173-188

Ghosh et al., 2009

S. Ghosh, Z.-Y. Wang, S. Kang, P.C. Bhowmik, B.S. Xing **Sorption and fractionation of a peat derived humic acid by kaolinite, montmorillonite, and goethite**

Pedosphere, 19 (2009), pp. 21-30

Henneberry et al., 2012

Y.K. Henneberry, T.E.C. Kraus, P.S. Nico, W.R. Horwath **Structural stability of coprecipitated natural organic matter and ferric iron under reducing conditions**

Org. Geochem., 48 (2012), pp. 81-89

Hernes et al., 2013

P.J. Hernes, K. Kaiser, R.Y. Dyda, C. Cerli **Molecular trickery in soil organic matter: hidden lignin**

Environ. Sci. Technol., 47 (2013), pp. 9077-9085

Jagadamma et al., 2012

S. Jagadamma, M.A. Mayes, J.R. Phillips **Selective sorption of dissolved organic carbon compounds by temperate soils**

PLoS One, 7 (2012)

Jobbagy and Jackson, 2000

E.G. Jobbagy, R.B. Jackson **The vertical distribution of soil organic carbon and its relation to climate and vegetation**

Ecol. Appl., 10 (2000), pp. 423-436

Jones and Edwards, 1998

D.L. Jones, A.C. Edwards **Influence of sorption on the biological utilization of two simple carbon substrates**

Soil Biol. Biochem., 30 (1998), pp. 1895-1902

Kaiser and Guggenberger, 2000

K. Kaiser, G. Guggenberger **The role of DOM sorption to mineral surfaces in the preservation of organic matter in soils**

Org. Geochem., 31 (2000), pp. 711-725

Kaiser and Guggenberger, 2007

K. Kaiser, G. Guggenberger **Sorptive stabilization of organic matter by microporous goethite: sorption into small pores vs. surface complexation**

Eur. J. Soil Sci., 58 (2007), pp. 45-59

Kaiser et al., 2007

K. Kaiser, R. Mikutta, G. Guggenberger **Increased stability of organic matter sorbed to ferrihydrite and goethite on aging**

Soil Sci. Soc. Am. J., 71 (2007), pp. 711-719

Kalbitz et al., 2005

K. Kalbitz, D. Schwesig, J. Rethemeyer, E. Matzner **Stabilization of dissolved organic matter by sorption to the mineral soil**

Soil Biol. Biochem., 37 (2005), pp. 1319-1331

Keiluweit et al., 2015

M. Keiluweit, J.J. Bougoure, P.S. Nico, J. Pett-Ridge, P.K. Weber, M. Kleber  
**Mineral protection of soil carbon counteracted by root exudates**

Nat. Clim. Chang., 5 (2015), pp. 588-595

Kleber et al., 2015

M. Kleber, K. Eusterhues, M. Keiluweit, C. Mikutta, R. Mikutta, P.S. Nico (Eds.),  
Mineral-organic Associations: Formation, Properties, and Relevance in Soil  
Environments, Elsevier, Amsterdam (2015)

Kogel-Knabner et al., 2008

I. Kogel-Knabner, G. Guggenberger, M. Kleber, E. Kandeler, K. Kalbitz, S. Scheu,  
K. Eusterhues, P. Leinweber  
**Organo-mineral associations in temperate soils: integrating biology, mineralogy, and organic matter chemistry**

J. Plant Nutr. Soil Sci.-Zeitschrift Fur Pflanzenernahrung Und Bodenkunde, 171 (2008), pp. 61-82

Lalonde et al., 2012

K. Lalonde, A. Mucci, A. Ouellet, Y. Gelin  
**Preservation of organic matter in sediments promoted by iron**

Nature, 483 (2012), pp. 198-200

Lawrence et al., 2015

C.R. Lawrence, J.W. Harden, X.M. Xu, M.S. Schulz, S.E. Trumbore  
**Long-term controls on soil organic carbon with depth and time: a case study from the Cowlitz River chronosequence, WA USA**

Geoderma, 247 (2015), pp. 73-87

Lehmann and Kleber, 2015

J. Lehmann, M. Kleber  
**The contentious nature of soil organic matter**

Nature, 528 (2015), pp. 60-68

Lynch and Wojciechowski, 2015

J.P. Lynch, T. Wojciechowski  
**Opportunities and challenges in the subsoil: pathways to deeper rooted crops**

J. Exp. Bot., 66 (2015), pp. 2199-2210

Masiello et al., 2004

C.A. Masiello, O.A. Chadwick, J. Southon, M.S. Torn, J.W. Harden  
**Weathering controls on mechanisms of carbon storage in grassland soils**

Glob. Biogeochem. Cycles, 18 (2004)

Mayes et al., 2012



M.A. Mayes, K.R. Heal, C.C. Brandt, J.R. Phillips, P.M. Jardine **Relation between soil order and sorption of dissolved organic carbon in temperate subsoils**

Soil Sci. Soc. Am. J., 76 (2012), pp. 1027-1037

Mikutta et al., 2006

R. Mikutta, M. Kleber, M.S. Torn, R. Jahn **Stabilization of soil organic matter: association with minerals or chemical recalcitrance?**

Biogeochemistry, 77 (2006), pp. 25-56

Mikutta et al., 2007

R. Mikutta, C. Mikutta, K. Kalbitz, T. Scheel, K. Kaiser, R. Jahn **Biodegradation of forest floor organic matter bound to minerals via different binding mechanisms**

Geochim. Cosmochim. Acta, 71 (2007), pp. 2569-2590

Olsson et al., 2011

R. Olsson, R. Giesler, P. Persson **Adsorption mechanisms of glucose in aqueous goethite suspensions**

J. Colloid Interface Sci., 353 (2011), pp. 263-268

Porras et al., 2017

R.C. Porras, C.E. Hicks Pries, K.J. McFarlane **Biogeochemistry**

133 (2017), p. 133, 10.1007/s10533-017-0337-6

Peters et al., 2012

G.P. Peters, G. Marland, C. Le

Quere, T. Boden, J.G. Canadell, M.R. Raupach **Rapid growth in CO<sub>2</sub> emissions after the 2008-2009 global financial crisis**

Nat. Clim. Chang., 2 (2012), pp. 2-4

Raich and Schlesinger, 1992

J.W. Raich, W.H. Schlesinger **The global carbon-dioxide flux in soil respiration and its relationship to vegetation and climate**

Tellus Ser. B Chem. Phys. Meteorol., 44 (1992), pp. 81-99

Riley et al., 2014

W.J. Riley, F. Maggi, M. Kleber, M.S. Torn, J.Y. Tang, D. Dwivedi, N. Guerry **Long residence times of rapidly decomposable soil organic matter: application of a multi-phase, multi-component, and vertically resolved model (BAMS1) to soil carbon dynamics**

Geosci. Model Dev., 7 (2014), pp. 1335-1355

Rumpel and Kogel-Knabner, 2011

C. Rumpel, I. Kogel-Knabner **Deep soil organic matter—a key but poorly understood component of terrestrial C cycle**

Plant Soil, 338 (2011), pp. 143-158

Salome et al., 2010

C. Salome, N. Nunan, V. Pouteau, T.Z. Lerch, C. Chenu **Carbon dynamics in topsoil and in subsoil may be controlled by different regulatory mechanisms**

Glob. Chang. Biol., 16 (2010), pp. 416-426

Scheel et al., 2007

T. Scheel, C. Dorfler, K. Kalbitz **Precipitation of dissolved organic matter by aluminum stabilizes carbon in acidic forest soils**

Soil Sci. Soc. Am. J., 71 (2007), pp. 64-74

Schmidt et al., 2011

M.W.I. Schmidt, M.S. Torn, S. Abiven, T. Dittmar, G. Guggenberger, I.A. Janssens, M. Kleber, I. Kogel-Knabner, J. Lehmann, D.A.C. Manning, P. Nannipieri, D. P. Rasse, S. Weiner, S.E. Trumbore **Persistence of soil organic matter as an ecosystem property**

Nature, 478 (2011), pp. 49-56

Schneider et al., 2010

M.P.W. Schneider, T. Scheel, R. Mikutta, P. van Hees, K. Kaiser, K. Kalbitz **Sorptive stabilization of organic matter by amorphous Al hydroxide**

Geochim. Cosmochim. Acta, 74 (2010), pp. 1606-1619

Schwertmann and Cornell, 2007a

U. Schwertmann, R.M. Cornell **Ferrihydrite**

Iron Oxides in the Laboratory, Wiley-VCH Verlag GmbH (2007), pp. 103-112

Schwertmann and Cornell, 2007b

U. Schwertmann, R.M. Cornell **General preparative techniques**

Iron Oxides in the Laboratory, Wiley-VCH Verlag GmbH (2007), pp. 19-25

Schwertmann and Cornell, 2007c

U. Schwertmann, R.M. Cornell **Goethite**

Iron Oxides in the Laboratory, Wiley-VCH Verlag GmbH (2007), pp. 67-92

Shimizu et al., 2013

M. Shimizu, J. Zhou, C. Schroeder, M. Obst, A. Kappler, T. Borch **Dissimilatory reduction and transformation of ferrihydrite-humic acid coprecipitates**

Environ. Sci. Technol., 47 (2013), pp. 13375-13384

Sposito, 2008

G. Sposito **The Chemistry of Soils**

Oxford University Press, New York (2008)

Sutton and Sposito, 2005

R. Sutton, G. Sposito **Molecular structure in soil humic substances: the new view**

Environ. Sci. Technol., 39 (2005), pp. 9009-9015

Tarnocai et al., 2009

C. Tarnocai, J.G. Canadell, E.A.G. Schuur, P. Kuhry, G. Mazhitova, S. Zimov **Soil organic carbon pools in the northern circumpolar permafrost region**

Glob. Biogeochem. Cycles, 23 (2009)

Tipping, 1981

E. Tipping **The adsorption of aquatic humic substances by iron-oxides**

Geochim. Cosmochim. Acta, 45 (1981), pp. 191-199

Torn et al., 1997

M.S. Torn, S.E. Trumbore, O.A. Chadwick, P.M. Vitousek, D.M. Hendricks **Mineral control of soil organic carbon storage and turnover**

Nature, 389 (1997), pp. 170-173

Vogel et al., 2014

C. Vogel, C.W. Mueller, C. Hoschen, F. Buegger, K. Heister, S. Schulz, M. Schlotter, I. Kogel-Knabner **Submicron structures provide preferential spots for carbon and nitrogen sequestration in soils**

Nat. Commun., 5 (2014)